STAT3 Sensitizes Insulin Signaling by Negatively Regulating Glycogen Synthase Kinase-3β

Akira Moh,[1,2,3] Wenjun Zhang,[1,2] Sidney Yu,[3] Jun Wang,[1,2] Xuming Xu,[3] Jiliang Li,[4] and Xin-Yuan Fu[1,2,3]

OBJECTIVE—Glucose homeostasis is achieved by triggering regulation of glycogen synthesis genes in response to insulin when mammals feed, but the underlying molecular mechanism remains largely unknown. The aim of our study was to examine the role of the signal transducers and activators of transcription 3 (STAT3) in insulin signaling.

RESEARCH DESIGN AND METHODS—We generated a strain of mice carrying a targeted disruption of *Stat3* gene in the liver (*L-Stat3*$^{-/-}$ mice). Hepatocytes of the *L-Stat3*$^{-/-}$ mice were isolated to establish cell lines for mechanistic studies. Nuclear translocation and DNA-protein interaction of STAT3 was analyzed with immunofluorescent and chromatin immunoprecipitation methods, respectively. Levels of glucose, insulin, leptin, and glucagon were profiled, and putative downstream molecules of STAT3 were examined in the presence of various stimuli in *L-Stat3*$^{-/-}$ and control mice.

RESULTS—STAT3 was found to sensitize the insulin signaling through suppression of GSK-3β, a negative regulator of insulin signaling pathway. During feeding, both mRNA and protein levels of GSK-3β decreased in *Stat3*$^{f/+}$ mice, which reflected the need of hepatocytes for insulin to induce glycogen synthesis. In contrast, the *L-Stat3*$^{-/-}$ mice lost this control and showed a monophasic increase in the GSK-3β level in response to insulin. Administration of GSK-3β inhibitors lithium chloride and L803-mts restored glucose homeostasis and rescued the glucose intolerance and impaired insulin response in *L-Stat3*$^{-/-}$ mice.

CONCLUSIONS—These data indicate that STAT3 sensitizes insulin signaling by negatively regulating GSK-3β. Inactivation of STAT3 in the liver contributes significantly to the pathogenesis of insulin resistance. ***Diabetes*** **57:1227–1235, 2008**

From the [1]Department of Microbiology and Immunology, Indiana University School of Medicine, Indianapolis, Indiana; the [2]Walther Oncology Center, Indiana University School of Medicine, Indianapolis, Indiana; the [3]Department of Pathology, Yale University School of Medicine, New Haven, Connecticut; and the [4]Department of Biology, Indiana University–Purdue University Indianapolis, Indianapolis, Indiana.

Corresponding author: Xin-Yuan Fu, PhD, or Akira Moh, MD, PhD, Department of Microbiology and Immunology, Indiana University School of Medicine, 635 Barnhill Dr. MS 420, Indianapolis, IN 46202. E-mail: xfu@iupui.edu or amoh@iupui.edu.

Received for publication 12 November 2006 and accepted in revised form 4 February 2008.

Published ahead of print at http://diabetes.diabetesjournals.org on 11 February 2008. DOI: 10.2337/db06-1582.

Additional information for this article can be found in an online appendix at http://dx.doi.org/10.2337/db06-1582.

DAPI, 4′,6-diamidino-2-phenylindole; DMEM, Dulbecco's modified Eagle's medium; FBS, fetal bovine serum; GSK, glycogen synthase kinase; IL, interleukin; IRS, insulin receptor substrate; STAT, signal transducers and activators of transcription; TTR, transthyretin.

The hallmark of type 2 diabetes, the most common metabolic disorder, is a defect in the insulin-signaled glucose metabolism of peripheral tissues, a phenomenon defined as insulin resistance. Physiologically, insulin signals through a pathway involving protein kinases including, but not limited to, phosphatidylinositol 3-kinase, AKT or protein kinase B (PKB), and glycogen synthase kinase (GSK)-3β (the phosphatidylinositol 3-kinase/Akt/GSK-3β pathway) (1).

Unlike the other members of the pathway, GSK-3β is a key negative regulator in insulin signaling (2). GSK-3β is a ubiquitous cytosolic serine/threonine protein kinase that has been implicated in multiple receptor-mediated intracellular processes (3). The unique feature that distinguishes GSK-3β from other protein kinases is that it is constitutively active in resting conditions and acts as a suppressor in the insulin signaling pathway (2). The fact that the function of two key targets of insulin action, glycogen synthase and insulin receptor substrate-1 (IRS-1), are suppressed by GSK-3β (4–6) and the fact that GSK-3β activity is higher in diabetic tissues (7) make it a promising drug discovery target for insulin resistance and type 2 diabetes.

Signal transducers and activators of transcription (STAT) proteins comprise a family of transcription factors latent in the cytoplasm that consists of seven different members: STAT1, -2, -3, -4, -5A, -5B, and -6 (8,9). Unlike all other members of the STAT gene family, the ablation of STAT3 leads to embryonic lethality (10). This finding, along with evidence of its activation by a wide variety of cytokines, growth factors, and other stimuli (11,12), implies that STAT3 might be more generally deployed than its relatives and suggests that it might represent a primordial STAT protein.

It is now clear that STATs can be activated to participate in gene control when cells encounter various noncytokine polypeptides (13). Earlier studies have shown that STAT3 could be phosphorylated by insulin in vitro (14,15). However, the biological effect of the activation remains unknown, probably due to the lack of an animal model resulting from embryonic lethality in generalized STAT3 ablation. Recently, other investigators and our group have succeeded in removing STAT3 from individual tissue by the Cre/LoxP method (16), which circumvents the problem of embryonic lethality and has demonstrated roles for STAT3 in a wide variety of tissues (17). Interestingly, liver-specific ablation of STAT3 led to an increase in hepatic gluconeogenic genes and insulin resistance, which was attributed to the disruption of interleukin-6 (IL6) signaling either directly (18) or through a brain-mediated release of IL6 from the liver (19). However, the role of STAT3 in insulin signaling per se is still not clear. The aim

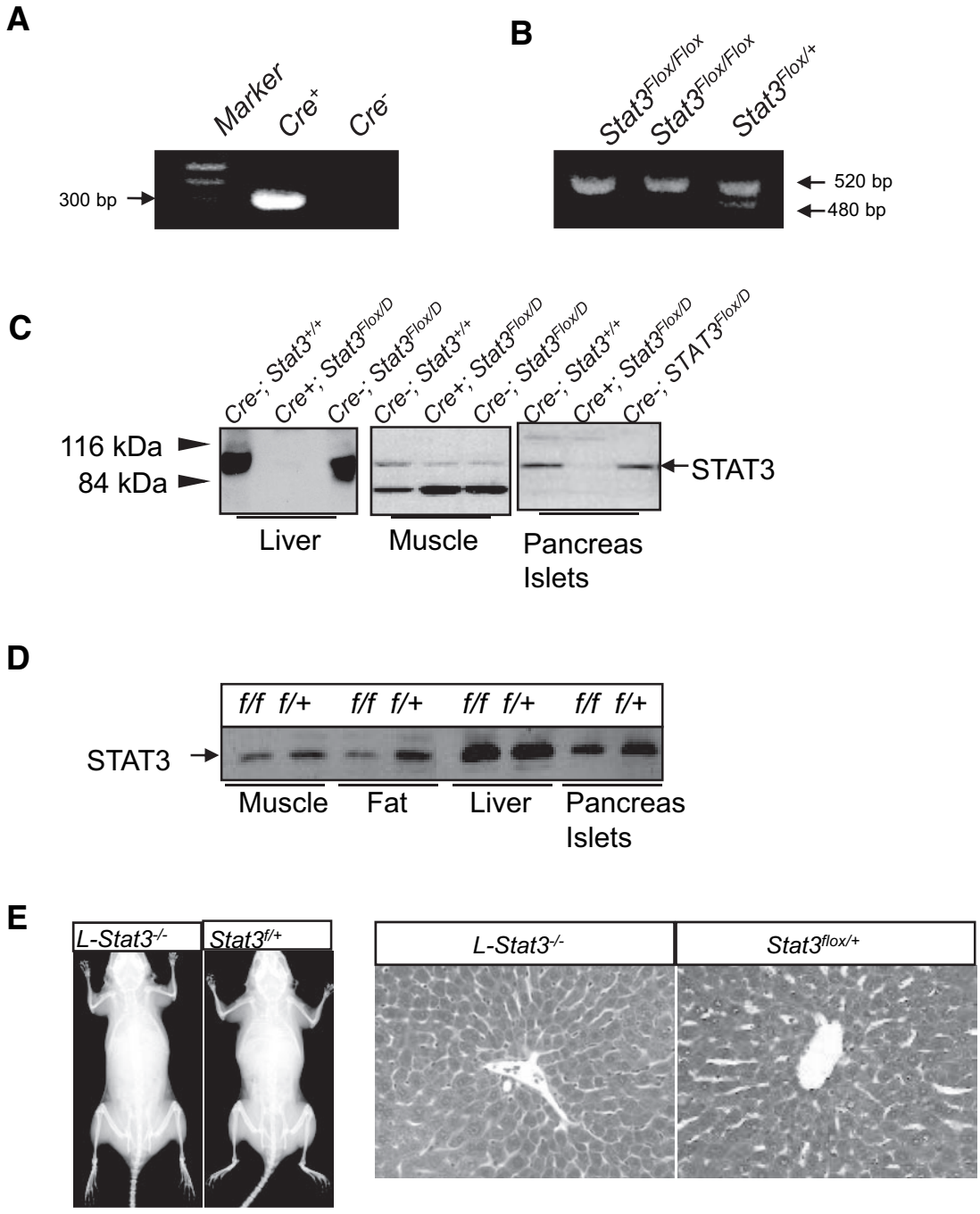

FIG. 1. Background data for generation of the liver *Stat3*$^{-/-}$ (*L-Stat3*$^{-/-}$) mice. *A*: Genotyping of the *Ttr-Cre*. The *Ttr-Cre* transgene was detected with the primers amplifying a 300-bp fragment. *B*: The *Stat3*^{flox} allele was detected with the primers amplifying a 520-bp fragment, while *Stat3* wild-type allele gave 480-bp fragment. *C*: Western blot analysis of STAT3 protein in the liver, muscle, and pancreatic islets of line 10-3 *L-Stat3*$^{-/-}$ and littermate control mice. *D*: Western blot of STAT3 in major metabolic organs of control mice with different alleles of *Stat3*. *E*: Representative X-ray picture of *L-Stat3*$^{-/-}$ and control mice (*left panel*). Hematoxylin-eosin (H-E) staining of *L-Stat3*$^{-/-}$ and *Stat3*$^{f/+}$ littermate control mice (*right panel*). Original magnification ×40.

of our study was to examine the primary role of STAT3 in insulin signaling in these gene-targeted mice. We found that STAT3 contributes to sensitizing insulin signaling by negatively regulating GSK-3β, which is a key negative regulator of insulin signaling (2).

RESEARCH DESIGN AND METHODS

Generation of transgenic mice expressing Cre-recombinase in the liver. Details of generating the transthyretin (*Ttr*) transgenic mice are described in a previous study by Moh et al. (16). Briefly, vector *Ttr*1ExV3, which contains the upstream transcriptional regulation region, the first exon and intron, and a partial second exon of the *Ttr* gene (20), was digested with *Stu*I. A fragment containing the open reading frame of the Cre gene was recovered from the mammalian expression vector pBS185 (GIBCO BRL, Life Technologies, Grand Island, NY) by digestion with *Xho*I and *Mlu*I and inserted into the *Stu*I site of *Ttr*1ExV3 to get the final construct p*Ttr-Cre*. The plasmid p*Ttr-Cre* was digested with *Hin*dIII to generate a transgene fragment, which was isolated by agarose gel electrophoresis. The purified transgene fragment was injected into fertilized eggs as described previously (21).

Creation and genotyping of tissue specific *L-Stat3*$^{-/-}$ mice in the liver. Generation of mice with a conditional *Stat3* allele has been described previously (22). Exons 18–20, which contained the SH2 domain of *Stat3*, were flanked by two loxP sites (*Stat3*$^{f/f}$). Two *Ttr-Cre* transgenic mouse strains

TABLE 1
Phenotypes of *L-Stat3*$^{-/-}$ and littermate controls*

	Stat3$^{+/+}$	*Stat3*$^{+/+}$;Cre	*StatT3*$^{f/+}$;Cre	*Stat3*$^{f/f}$;Cre
Body weight (g)	24.88 ± 1.64	24.14 ± 1.61	23.99 ± 1.59	24.34 ± 1.67
Fat mass (g)	4.27 ± 0.34	4.15 ± 0.29	4.12 ± 0.31	4.25 ± 0.36
Lean mass (g)	19.51 ± 0.97	18.98 ± 0.92	18.96 ± 0.91	19.28 ± 0.98
% Body fat	15.12 ± 0.77	15.25 ± 0.83	15.26 ± 0.74	15.54 ± 0.81
Blood glucose (mg/dl)				
Fasting	106.7 ± 15.8	107.3 ± 15.6	104.7 ± 14.9	119.6 ± 16.1
Feeding	117.8 ± 17.1	112.7 ± 16.3	116.7 ± 16.9	121.9 ± 18.4
Serum insulin (ng/dl)				
Fasting	0.51 ± 0.38	0.52 ± 0.32	0.48 ± 0.29	0.45 ± 0.17
Feeding	0.64 ± 0.45	0.58 ± 0.37	0.46 ± 0.28	0.49 ± 0.14
HOMA-IR	54.42 ± 6.00	55.80 ± 4.99	50.26 ± 4.32	53.8 ± 2.73
Serum leptin (ng/ml)	7.06 ± 1.39	6.98 ± 1.37	7.15 ± 1.48	10.41 ± 3.52

Data are means ± SD. n = 4–6 for each group. *Male mice measured during 8–12 weeks of age. HOMA-IR, homeostasis model assessment of insulin resistance.

(10-3 and 19-1) were crossed with *Stat3*$^{f/f}$ mice. The genotype was determined by PCR as described previously (22). Mice for experiments were produced by the breeding of male *Stat3*$^{f/+}$;*Cre* and female *Stat3*$^{f/+}$ in most cases or *Stat3*$^{f/f}$ in some occasions. Male *L-Stat3*$^{-/-}$ and littermate *Stat3*$^{f/+}$ control mice at the age of 8–12 weeks were used for experiments.

Hepatocyte culture, immortalization, and insulin treatment. Hepatocytes were isolated by in situ perfusion as previously described (23) with minor modifications. Briefly, the liver was perfused with 0.5 mmol/l EGTA and 0.15 g/l collagenase via the inferior cava. After perfusion, the dissociated liver was minced and suspended in Hanks' balanced salt solution. Cells were centrifuged twice at 500*g*, and hepatocytes were separated by centrifugation through a Percoll layer. Cells were counted and plated onto 10-cm dishes with 2×10^6 cells. Three cell lines were established by immortalization of hepatocytes from *L-Stat3*$^{-/-}$ and littermate wild-type mice with simian virus 40 T antigen. The cell lines were screened for STAT3 and hepatocyte markers. Line 2F4 of STAT3-null hepatocytes was used in most experiments, and results were confirmed with the other two lines. All hepatocytes were cultured in 4.5 g/l Dulbecco's modified Eagle's medium (DMEM; high glucose) enriched with 10% fetal bovine serum (FBS). After serum starvation for 4 h, 100 nmol/l insulin was added to 80% confluent hepatocytes. The cells were scalped and collected at the indicated time point after being washed with PBS three times.

Cell transfection. The plasmid constructs of *Stat3* were gifts from Dr. JE Darnell of Rockefeller University. The *Stat3-CA* construct was made by substituting cysteine residues for A661 and N663 of murine *Stat3*. This renders the STAT3-CA molecule capable of dimerizing without a phosphate on tyrosine 705 (24). *Stat3-S727A* was made by substituting alanine for serine 727 of STAT3. For transfection, cell lines of hepatocytes were transfected with Lipofectamine 2000 according to manufacture's instruction (Invitrogen, Carlsbad, CA). Cells were cultured for 48–72 h until harvesting.

Tissue and cell extraction for immunoblotting. Homogenized mouse liver (100 mg) and cultured hepatocytes were lysed in a whole-cell extraction buffer (400 mmol/l KCl, 10 mmol/l $NaHPO_4$,1 mmol/l EDTA, 1 mmol/l dithiothreitol, 10% [w/v] glycerol, 1 μg/ml aprotinin, 1 μg/ml leupeptin, 1 μg/ml pepstatin, 1 mmol/l phenylmethylsulfonyl fluoride, 5 mmol/l NaF, and 1 mmol/l Na_3VO_4). After centrifugation at 14,000 rpm, the supernatant was collected, and protein concentration was quantified with the BCA kit (Pierce, Rockford, IL). Ten micrograms of proteins were separated by SDS-polyacrylamide gel electrophoresis and then transferred to an Immuno-Blot polyvinylidene difluoride membrane (Bio-Rad, Hercules, CA). After blocking with 5% nonfat milk in a washing buffer (10 mmol/l Tris-HCl, 150 mmol/l NaCl, 1 mmol/l EDTA, and 0.1% [w/v] Triton X-100, pH 8.0), the membranes were soaked in the indicated antibodies, followed by soaking in anti-rabbit or anti-mouse IgG coupled with horseradish peroxidase and visualized using SuperSignal Chemiluminescent Substrate (Pierce).

Chromatin immunoprecipitation assay. Cell line of STAT3-null hepatocytes (line 2F4) was used for the chromatin immunoprecipitation assay. Different forms of *Stat3* (wild-type *Stat3*, *Stat3CA*, and *Stat3 S727A*) were reintroduced to the hepatocyte by transfection. The cells were cultured in DMEM with 10% FBS for 72 h. After incubation with 100 nmol/l insulin for 2 h, the cells were collected for immunoprecipitation assay with standard procedures as described previously (25). Specific antibodies against STAT3 provided by Dr. Zhong Zhong (26) were used for the immunoprecipitation. Normal rabbit IgG served as a negative control. For PCR, 1 μl from 50 μl precipitated DNA fragments was analyzed with 21–25 cycles of amplification using primers P1 (NT_039624, forward, 5′-GATCCTTCCGCCGCTTCCCT-3′) and P2 (NT_039624, backward, 5′-AAGACTTCGTTCTCTTGGCT-3′) directed against the mouse GSK-3β regulation region or a cytoplasmic β-actin coding region of the 1st exon as a negative control (NT_039324, forward, 5′-GTCAGAAGGACTCCTATGTG-3′; backward, 5′-GGCGTGGCTGAGAAGCTG-3′).

Luciferase assay. All of the different *stat3* constructs were subcloned into pcDNA3 plasmid. A total of 400 ng DNA was transfected into STAT3-null hepatocytes (line 2F4). Mouse *Gsk-3β* gene promoter region from nucleotides −584 to +1,459 was amplified from mouse genomic DNA by PCR using *Gsk-3β* promoter sequence–specific primers with *Xho*I and *Hin*dIII adaptation sites in 5′ and 3′ primers, respectively (sense, 5′-CCGCTCGAGTCGGCTCGG AAAGCAGATG-3′; antisense, 5′-CCCAAGCTTCGTTCTCTTGGCTTTTCACTC-3′), and subcloned into PGL3-Basic luciferase reporter plasmid (Promega). For transient transfection, 80% confluent cells in a 24-well plate were transfected with *Gsk-3β* promoter-luciferase construct and pCMV β-galactosidase or in combination with wild-type or different *Stat3* expression plasmids, or control vector using Lipofectamine 2000 (Invitrogen). Luciferase activity was assayed 24 h after transfection using the Dual-light luciferase kit (Applied Bioscience). Values were normalized with β-galactosidase activity expressed from pCMV β-galactosidase plasmid (Clontech).

Quantitative RT-PCR analysis of liver mRNA. RNA was extracted from the liver or hepatocytes using a TRIzol reagent (Invitrogen Life Technologies, Carlsbad, CA) following the manufacturer's instructions. Total RNA (2 μg) was used to prepare cDNA (iScript cDNA synthesis kit; Bio-Rad) using random hexamers. cDNA was amplified by PCR with a iQ SYBR Green Supermix kit (Bio-Rad). The primers are GSK-3β (NM_019827, forward, 5′-CACTCAAGAACTGTCAAGTAAC-3′, and reverse, 5′-CATTAGTATCTGAGG CTGCTG-3′) located at the two joints of the last three exons; PEPCK (forward, GTGTCATCCGCAAGCTGAAG, and backward, CTTTCGATCCTGG CCACATC) (27); glucose-6-phosphatose (G6Pase) (forward, CTGCAAGG GAGAACTCAGCAA, and backward, GAGGACCAAGGAAGCCACAAT) (27); and peroxisome proliferator–activated receptor-γ coactivator (PGC-1α) (forward, 5′-ATACCGCAAAGAGCACGAGAAG-3′, and backward, 5′-CTCAAGAG CAGCGAAAGCGTCACAG-3′) (18). PCR conditions are as follows: one cycle of 94°C for 2 min; 35 cycles of 94°C for 30 s, 55°C for 30 s, and 72°C for 45 s; followed by one cycle of 72°C for 10 min. β-Actin cDNA was amplified as an internal control with the same condition (X03672, forward, 5′-CCAGAGCAA GAGAGGCATCC-3′, and backward, 5′-AGGTCTTTACGGATGTCAACG-3′; length 704 bp). All data were means of fold change of triplicate analysis and normalized with those of β-actin. The fold change represents the change of transcript levels in the liver/cells relative to *Stat3*$^{f/+}$ at time point 0 in a time course and to STAT3-null, nontreatment control in transfection experiments after normalization with β-actin levels.

Histological and immunofluorescent staining. For hematoxylin-eosin (H-E), the sections were prepared and sent to Yale Pathological Services for H-E staining. For immunofluorescent staining, the sections were incubated with rabbit antibody against phosphorylated STAT3 (tyrosine 705 or serine 727) overnight at 4°C. The staining was visualized with a Rodamin-labeled donkey anti-rabbit second antibody (Jackson Immunoresearch Laboratories, West Grove, PA) under a fluorescent microscope. The nuclei were counterstained with 4′,6-diamidino-2-phenylindole (DAPI). Nuclear STAT3 was quantitated by the product of mean color level multiplied by the area in pixel. The ratio of intensity of each group to that of *L-Stat3*$^{-/-}$ at point 0 was calculated to normalize different stains and given as fold change in the figure.

Statistical analysis. Data are presented as mean ± SD. The difference of two genotype groups was analyzed by a Student's t test. Data in a time course

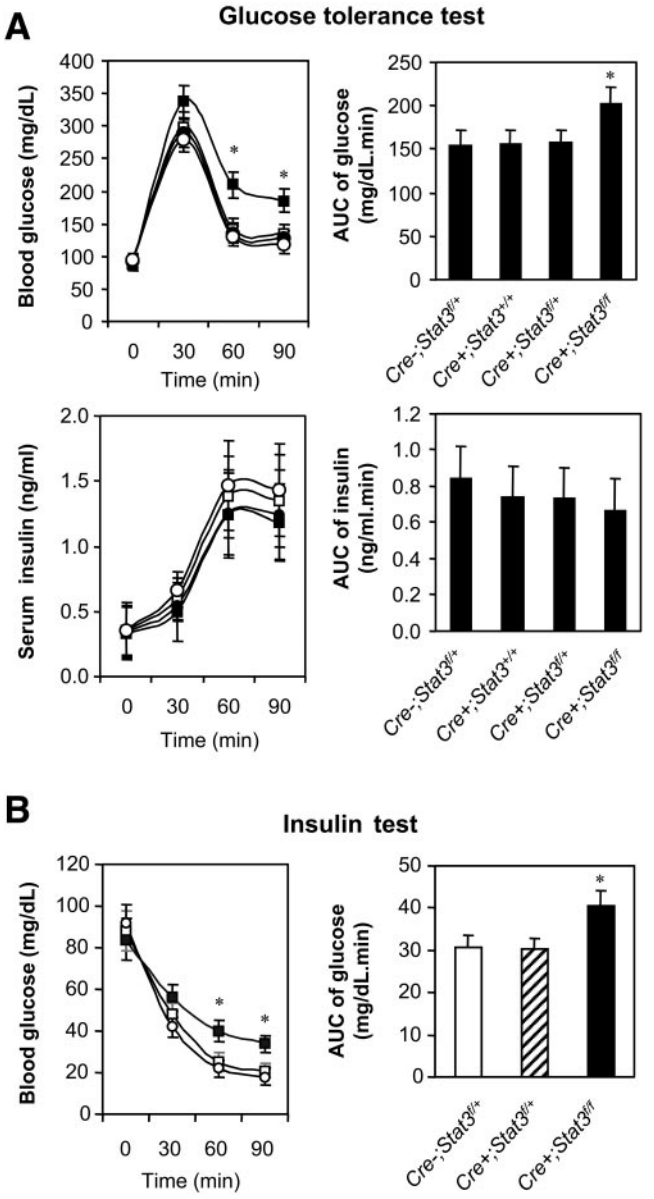

FIG. 2. Glucose intolerance and impaired insulin response in *L-Stat3*$^{-/-}$ mice. *A*: Glucose tolerance test. After overnight fasting, 2 g/kg glucose was injected into *L-Stat3*$^{-/-}$ mice and their littermate controls intraperitoneally. Glucose was measured at the indicated time points. ■, *L-Stat3*$^{-/-}$; ○, *Stat3*$^{f/+}$; ●, *Cre*+;*Stat3*$^{+/+}$; and □, *Cre*+; *Stat3*$^{f/+}$; $n = 6$ for each group. *B*: Insulin test. Exogenous insulin (bovine, 1 IU/kg) was injected intraperitoneally after overnight fasting. ■, *L-Stat3*$^{-/-}$; ○, *Stat3*$^{f/+}$; and □, *Cre*+;*Stat3*$^{f/+}$; $n = 7$ for each group. AUC, area under a curve. All data were means ± SD. *$P < 0.05$ between *L-Stat3*$^{-/-}$ and the rest of the groups by ANOVA.

experiment or over two groups were tested by one-way ANOVA. $P < 0.05$ was considered to be significant. Additional information is available in an online appendix at http://dx.doi.org/10.2337/db06-1582.

RESULTS

Generation of transgenic mice expressing Cre recombinase in the liver. We have generated three lines of transgenic mice with C57BL/6 background expressing the transgene that encodes the Cre recombinase enzyme under the control of the *Ttr* promoter (*Ttr-Cre*) in the liver. As shown in Fig. 1*A*, PCR amplified a 300-bp DNA band of the transgene encoding the Cre recombinase. We previously created mice carrying a *Stat3* allele with exons 18–20 flanked by *loxP* sites (*Stat3*$^{flox/flox}$ mice with genotyping shown in Fig. 1*B*) (22) and bred them with a line of *Ttr-Cre* transgenic mice. A deletion of exons 19 and 20, which encode the SH2 domain of *Stat3*, results in a conditional knockout of STAT3 protein in the liver (*L-Stat3*$^{-/-}$) and pancreatic islet (Fig. 1*C*). The basal level of STAT3 in the muscle was lower than other organs like the liver, and densitometry analysis did not show significant differences among the different forms of STAT3 in the muscle (Fig. 1*C*).

The *L-Stat3*$^{-/-}$ (*Ttr Cre*$^{+}$;*Stat3*$^{f/f}$) mice were born at a Mendelian rate and were otherwise normal (Table 1) except for impaired insulin signaling (see below). No significant morphological changes or inflammatory infiltration were noted in the livers of *L-Stat3*$^{-/-}$ mice (Fig. 1*E*). Young *L-Stat3*$^{-/-}$ mice did not develop obesity (Fig. 1*E*; Table 1), and even at 18 months of age (32.78 ± 1.98 vs. 32.66 ± 1.82 g body wt, *Stat3*$^{f/+}$ vs. *L-Stat3*$^{-/-}$ male mice, $n = 6$ for each group), there were no significant differences in fat mass between the two groups. No STAT3 deletion was found in the brain or fat tissue (not shown). The abundances of STAT3 protein in major metabolic organs did not differ between *Stat3*$^{f/f}$ and *Stat3*$^{f/+}$ (Fig. 1*D*), and *Stat3*$^{f/+}$ mice were used as controls for experiments.

Glucose intolerance and decreased insulin sensitivity in the *L-Stat3*$^{-/-}$ mice. Fasting blood glucose results (Table 1) in the *L-Stat3*$^{-/-}$ mice (line 10-3) were not significantly different from those of their littermates. However, glucose levels at 60 and 90 min in *L-Stat3*$^{-/-}$ mice were significantly higher than in their *Stat3*$^{f/+}$ littermates after 2 g/kg glucose was injected intraperitoneally (Fig. 2*A*). We delivered exogenous insulin (1 IU/kg i.p.) to examine the response in the *L-Stat3*$^{-/-}$ and littermate *Stat3*$^{f/+}$ mice. Glucose levels were significantly higher at 60 and 90 min in *L-Stat3*$^{-/-}$ mice than in their *Stat3*$^{f/+}$ littermates after insulin injection (Fig. 2*B*). The other line (19-1) of mice with STAT3 specifically knocked out in the liver had similar results (not shown). The glucose phenotypes of *Ttr-Cre*$^{+}$;*Stat3*$^{+/+}$ mice were similar to those of wild-type *Stat3* and *Stat3*$^{f/+}$ mice (not shown).

Nuclear translocation of STAT3 after insulin injection and inhibition of *Gsk-3β* gene promoter activity by constitutively active STAT3. Nuclear translocation of serine phosphorylated STAT3 (serine 727) was observed in vivo (Fig. 3*A*) and in vitro (Fig. 3*B*) after insulin treatment. Levels of tyrosine phosphorylated STAT3 (tyrosine 705) were also higher in the nuclei of *Stat3*$^{f/+}$ hepatocytes than those of *L-Stat3*$^{-/-}$ cells but did not show a significant increase after insulin treatment (Fig. 3). Bioinfomatic analysis revealed a relatively conserved STAT binding site in the gene promoter region of the *Gsk-3β* gene (Fig. 4*A*). Chromatin immunoprecipitation assay with a STAT3 antibody (26) and PCR amplification with primers covering the putative binding site revealed binding of STAT3 to the *Gsk-3β* regulation region (Fig. 4*C*). The binding was weakened by mutating serine 727 (Fig. 4*C*). The effect of STAT3 on *Gsk-3β* gene promoter activity was examined by luciferase assay. As shown in Fig. 4*D*, constitutively active STAT3 or STAT3 in the presence of insulin significantly inhibited *Gsk-3β* gene promoter activity, whereas serine 727 mutation abolished the inhibition (Fig. 4*D*). Quantitative RT-PCR analysis of mRNA confirmed that STAT3 CA or STAT3 in the presence of insulin suppressed *Gsk-3β* gene expression and that serine 727 might be important for the suppression (Fig. 4*E*). The suppression could be observed in the presence of cycloheximide (Fig. 4*E*).

Time course of GSK-3β mRNA in *L-Stat3*$^{-/-}$ and control mice after insulin injection is shown in Fig. 5*A*. Levels of

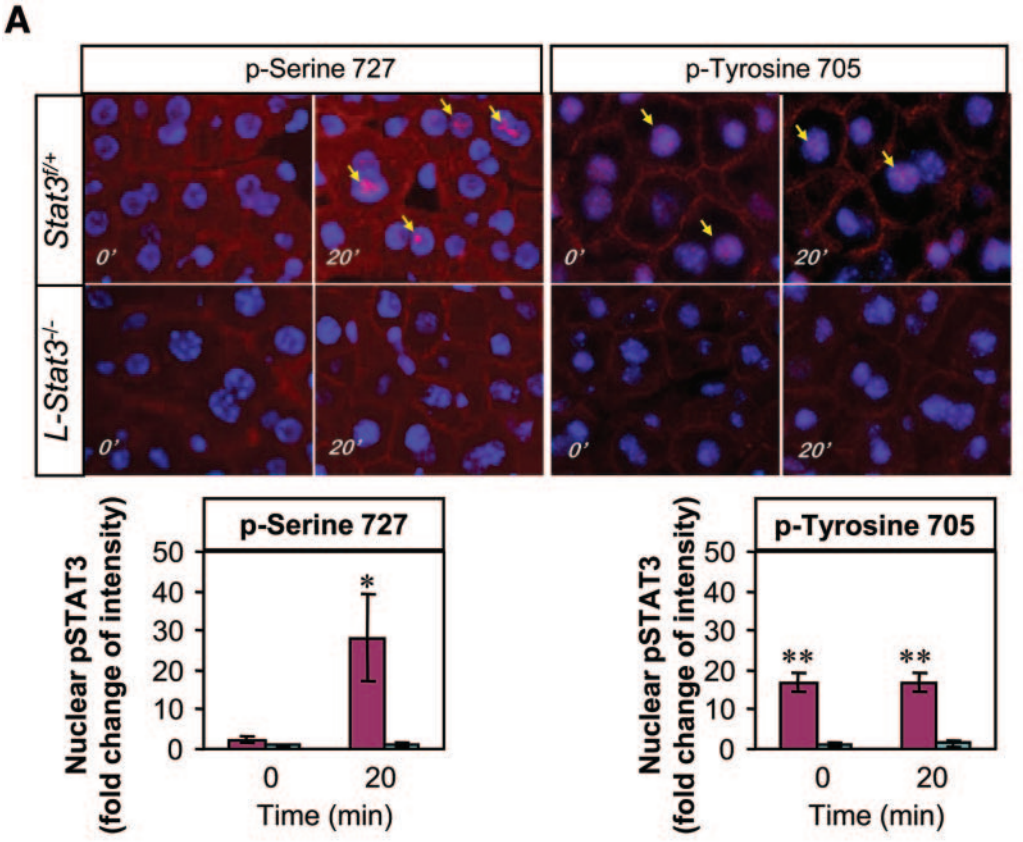

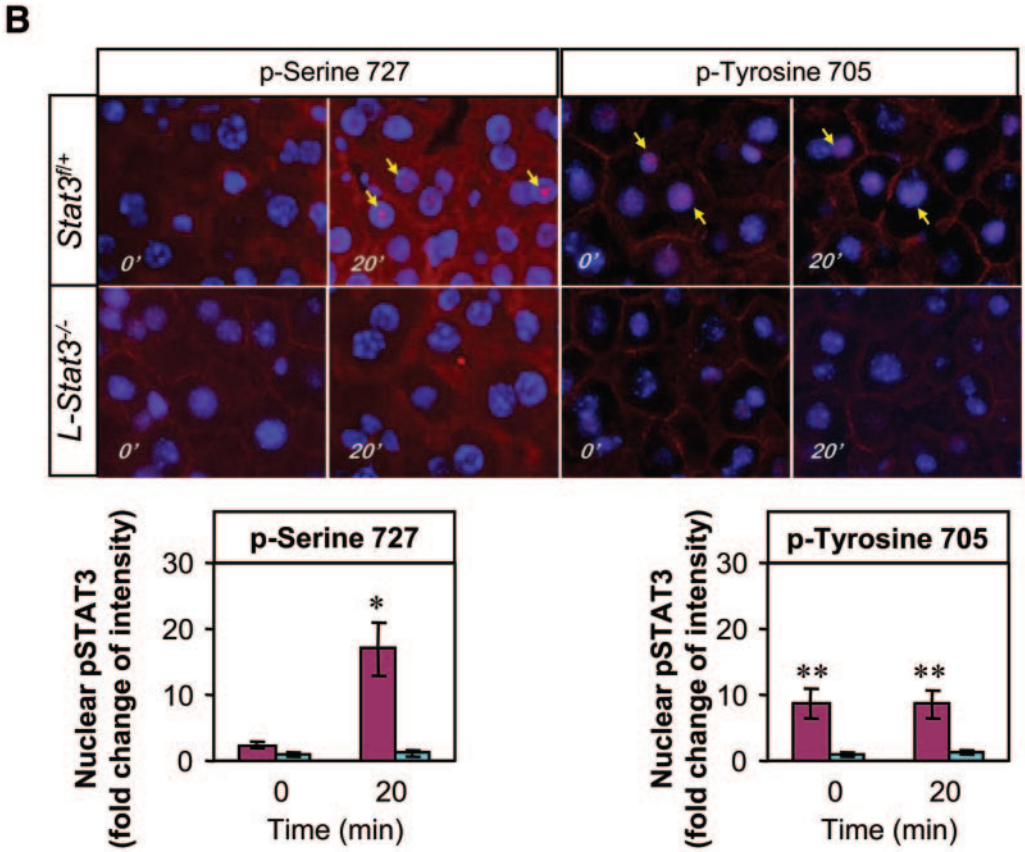

FIG. 3. Nuclear translocation of STAT3 after insulin treatment. The livers (*A*) or hepatocytes (*B*) of *L-Stat3*$^{-/-}$ and *Stat3*$^{fl/+}$ mice were removed or fixed after 0 (no insulin) and 20 min of insulin treatment. The liver sections or hepatocytes were stained with anti–phosphorylated STAT3 antibody (serine 727 or tyrosine 705 as indicated). Nuclei were stained with DAPI (blue). Positive staining of phosphorylated STAT3 (red) is indicated with yellow arrows. Numerals on the lower left corners of the microphotographs indicate time point of insulin treatment. Original magnification ×40. The intensity of phosphorylated STAT3 in the nuclei was the product of mean color level multiplied by the area. The ratio of intensity of each group to that of *L-Stat3*$^{-/-}$ at point 0 was calculated to normalize different stains and given as fold change in the figure. Dark red bars, *Stat3*$^{fl/+}$; cyan bars, *L-Stat3*$^{-/-}$. All numeral data were means ± SD of five mice in each group. *$P < 0.01$ between *L-Stat3*$^{-/-}$ and the rest of groups. **$P < 0.01$ between *L-Stat3*$^{-/-}$ and *Stat3*$^{fl/+}$.

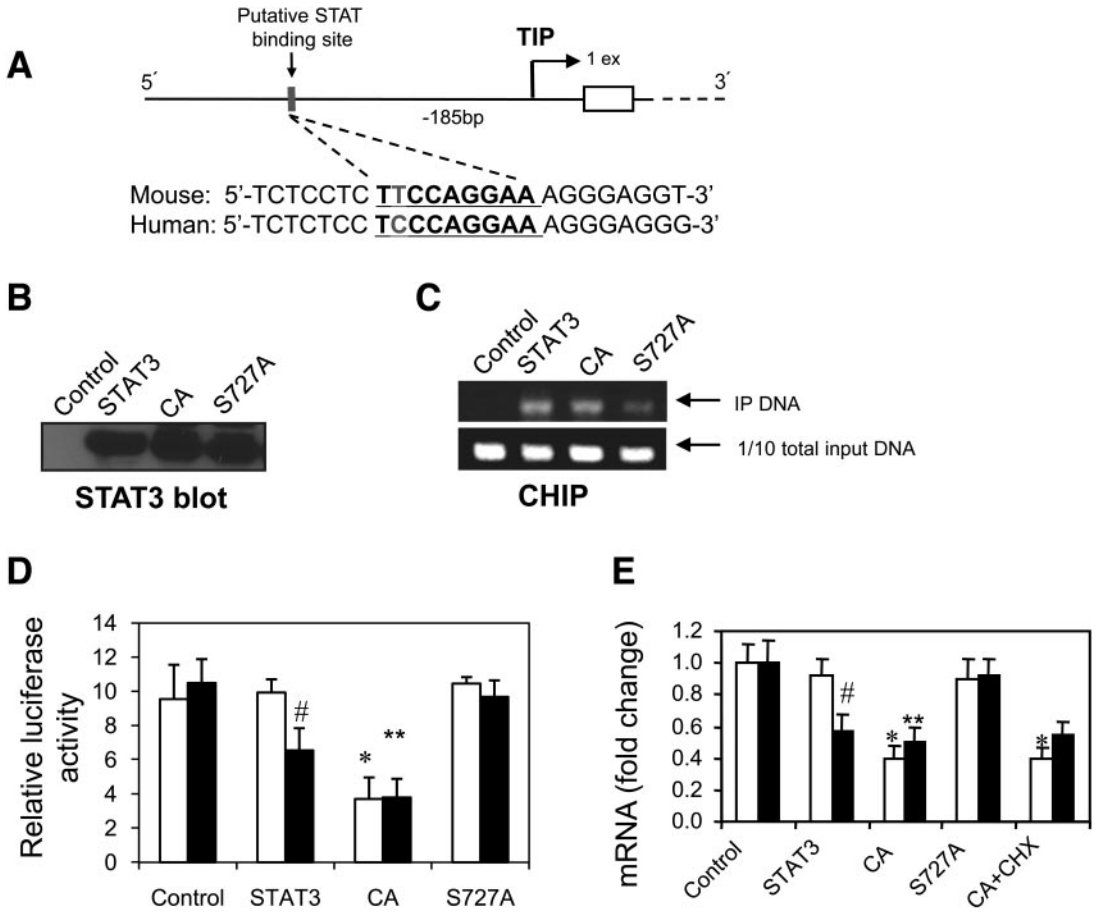

FIG. 4. Regulation of *Gsk-3β* gene by STAT3 in vitro. *A*: Simplified mouse *Gsk-3β* gene. TIP, transcriptional initiation point. The sequence of the putative STAT binding site is underlined. *B*: STAT3-null hepatocytes (cell line 2F4) were transfected with plasmid encoding wild-type *Stat3*, constitutively active (CA) *Stat3*, and *Stat3* mutant at serine 727 (S727A). Control was transfected with vector only, without *Stat3*. Cell lysate was collected and immunoblotted for STAT3. *C*: Nuclear lysate was prepared for chromatin immunoprecipitation (CHIP) from the transfected cells after incubation with 100 nmol/l insulin for 2 h. PCR amplified a 300-bp DNA fragment immunoprecipitated with a STAT3 antibody. Luciferase assay for *Gsk-3β* gene promoter activity (*D*) and mRNA expression (*E*) in the transfected hepatocytes. □, non–insulin treated; ■, insulin treated (100 nmol/l insulin for 2 h). For non–insulin-treated groups, *$P < 0.01$ between STAT3 CA or STAT3 CA+CHX and the rest of non–insulin-treated groups. For insulin-treated groups, **$P < 0.01$, STAT3 CA or STAT3 CA+CHX vs. control or STAT3 S727A of insulin-treated groups. For the groups with the same transfection, #$P < 0.05$ between non–insulin-treated STAT3 group and insulin-treated STAT3 group. CA, constitutively active; S727A, replacing serine 727 with alanine. CHX, 100 μg/ml cycloheximide. Please see RESEARCH DESIGN AND METHODS for details.

GSK-3β mRNA were significantly reduced in $Stat3^{f/+}$ mice at 30 and 60 min after insulin injection when compared with those of *L-Stat3*$^{-/-}$ mice. The reduction of the mRNA levels in $Stat3^{f/+}$ mice was stronger in feeding than in fasting condition (Fig. 5*A*).

GSK-3β protein tended to increase in *L-Stat3*$^{-/-}$ mice at randomly feeding (time point 0), but the difference was not statistically significant ($P = 0.067$) (Fig. 5*B*). Insulin injection induced a transient increase in both protein and phosphorylation levels of GSK-3β and a decrease after 30 min of insulin injection in the $Stat3^{f/+}$ control mice (Fig. 5*B*). In contrast, the GSK-3β level continuously increased after 30 min of insulin injection in the *L-Stat3*$^{-/-}$ mice (Fig. 5*B*). Similar results was present in fasting with lesser differences between the *L-Stat3*$^{-/-}$ and $Stat3^{f/+}$ mice than in feeding (Supplemental Fig. 2). After 30 min of insulin treatment, GSK-3β levels also increased in the *Stat3*$^{-/-}$ hepatocytes isolated from the liver of *L-Stat3*$^{-/-}$ mice (Fig. 5*C*). Similar pattern of GSK-3β in the *L-Stat3*$^{-/-}$ mice was present in glucose loading (Fig. 6*A*). Consistently, there was a significant reduction in glycogen synthase activity (Fig. 6*B*), but liver glycogen remained unchanged in the *L-Stat3*$^{-/-}$ mice after glucose loading (Fig. 6*C*).

Rescue the phenotype in *L-Stat3*$^{-/-}$ mice with a GSK-3β inhibitor, lithium chloride. It was clear that STAT3 deficiency in the liver led to an increase in GSK-3β expression. The next question we asked was whether or not the increased GSK-3β was responsible for the impaired insulin response in *L-Stat3*$^{-/-}$ mice. We treated *L-Stat3*$^{-/-}$ mice with lithium chloride, a GSK-3β blocker (28), before insulin injection. To avoid generalized effects of lithium and to obtain optimal results of GSK-3β inhibition, different doses and duration were tried. With the protocols given in Fig. 7, there were no significant differences in blood insulin level (Fig. 7*B*), mass of adipose tissue, and glycogen of skeletal muscle (not shown) between the *L-Stat3*$^{-/-}$ and control mice after lithium treatment. The impaired insulin signaling and glucose tolerance in *L-Stat3*$^{-/-}$ mice could be rescued by the GSK-3β inhibitor (Fig. 7*B* and *C*). Additional results are available in the online appendix.

DISCUSSION

Insulin resistance in liver STAT3–deficient lean mice and suppression of GSK-3β expression by STAT3. In the present work, we generated a strain of mice with *Stat3*

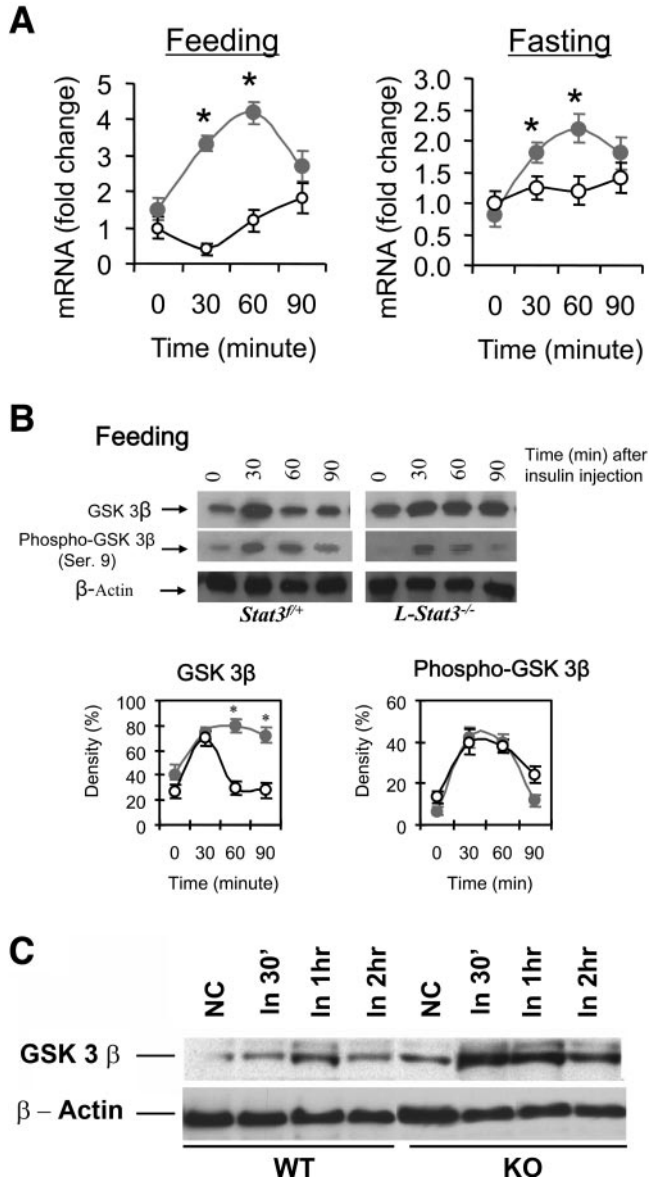

FIG. 5. Increase in GSK-3β mRNA and protein expression in *L-Stat3*$^{-/-}$ hepatocytes after insulin stimulation. *A*: The liver of *L-Stat3*$^{-/-}$ ($n = 5$) and *Stat3*$^{f/+}$ ($n = 5$) was removed at the indicated time point and RNA was extracted for quantitative RT-PCR assay. The fold change represents the change of transcript levels in the liver relative to *Stat3*$^{f/+}$ at time point 0 after normalization with β-actin levels. *$P < 0.01$ between *L-Stat3*$^{-/-}$ (●) and *Stat3*$^{f/+}$ (○) by ANOVA. *B*: Western blot analysis with GSK-3β and phosphorylated GSK-3β (Ser. 9) antibodies for samples collected from *A*. Densitometry curves for GSK-3β and phosphorylated GSK-3β were blotted from three experiments using the percentage of GSK-3β or phosphorylated GSK-3β to β-actin. ●, *L-Stat3*$^{-/-}$; ○, *Stat3*$^{f/+}$. *$P < 0.01$ between *L-Stat3*$^{-/-}$ and *Stat3*$^{f/+}$ by ANOVA. *C*: Hepatocytes were treated with insulin and cell lysates were collected for Western blot analysis at the indicated time point. NC, nontreated control. WT, *Stat3*$^{f/+}$. KO, *L-Stat3*$^{-/-}$. HC, hepatocyte.

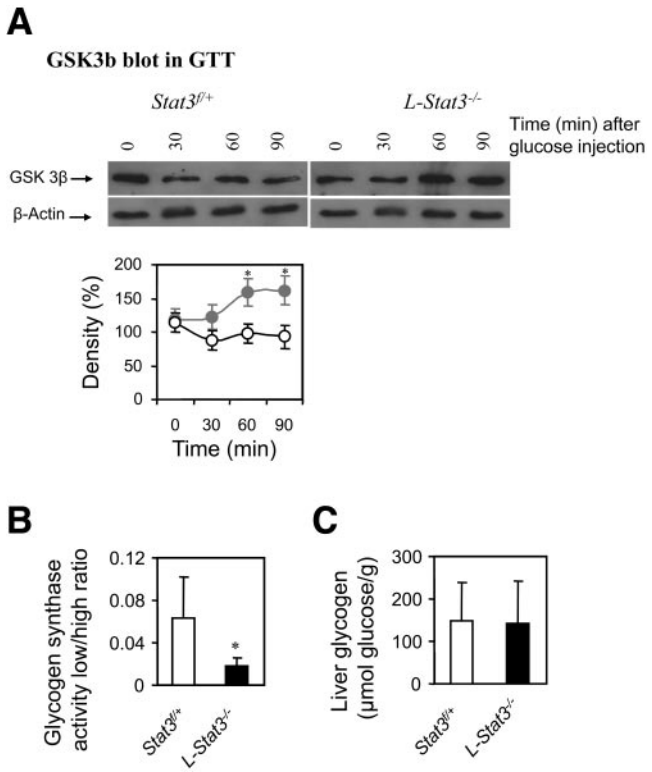

FIG. 6. GSK-3β, glycogen synthase, and glycogen levels after glucose loading. *A*: After overnight fasting, *L-Stat3*$^{-/-}$ and *Stat3*$^{f/+}$ mice were killed at the indicated time points after glucose injection (2 g/kg i.p.). The livers were collected for Western blot analysis with GSK-3β and β-actin antibodies. Densitometry curves for GSK-3β were blotted from three experiments using the percentage of GSK-3β to β-actin. ●, *L-Stat3*$^{-/-}$. ○, *Stat3*$^{f/+}$. *$P < 0.05$ between *L-Stat3*$^{-/-}$ and *Stat3*$^{f/+}$ by ANOVA. *B* and *C*: The livers at the end of the glucose injection (time point 90) were also used for glycogen synthase activity (*B*) and glycogen (*C*) assay. *$P < 0.05$ between *L-Stat3*$^{-/-}$ and *Stat3*$^{f/+}$ by *t* test.

gene being deleted in the liver and pancreatic islets (Fig. 1*C*). Insulin secretion in the *L-Stat3*$^{-/-}$ mice was not significantly affected by the islet deletion (Fig. 2*A*) as observed in Pdx-1 Cre mice with islet deletion of STAT3 (29), whereas early studies reported impaired insulin secretion in β-cell STAT3 deletion driven by RIP-Cre (30,31). Interestingly, the RIP-cre/*Stat3* phenotype results from hypothalamic, not islet, deletion of STAT3. The *L-Stat3*$^{-/-}$ mice demonstrated no obesity (Table 1) but significant insulin resistance (Fig. 2). These data clarify that STAT3 deficiency in the liver leads to primary insulin resistance. It is noteworthy that the serum leptin level tended to increase in the *L-Stat3*$^{-/-}$ mice (Table 1). This is consistent with previous findings in which insulin resistance in the liver increases the circulating levels of the extracellular domain of the leptin receptor, stabilizing leptin (32). It has been reported that STAT3 could be activated by insulin with some discrepancies as to whether tyrosine 705 or serine 727 or both were activated/phosphorylated (4,5,19). In the present study, the nuclear translocation of STAT3 was observed (Fig. 3*A* and *B*), implying that the activated STAT3 may be involved in a transcriptional event. We did a bioinformatic search, and *Gsk-3β* emerged as one candidate target gene with relatively conserved STAT3 binding site in the gene promoter region (Fig. 4*A*). Chromatin immunoprecipitation assay revealed that STAT3 was in the transcription complex associated with the STAT3 binding site (Fig. 4*C*). Luciferase assay demonstrated that constitutively active STAT3, which carries activated/phosphorylated serine 727 (24), inhibited the promoter activity of the *Gsk-3β* gene (Fig. 4*D*). The suppression was stronger in feeding than in fasting conditions (Fig. 5*A*).

The data were surprising because STAT3 is generally believed as a transcriptional activator. In some cases, the action of STAT3 seems to be ascribed to the induction of a set of important target genes, but in others, it may be acting as a repressor (e.g., in the thymic epithelium) (17,33) or as a signaling adaptor without a transcriptional

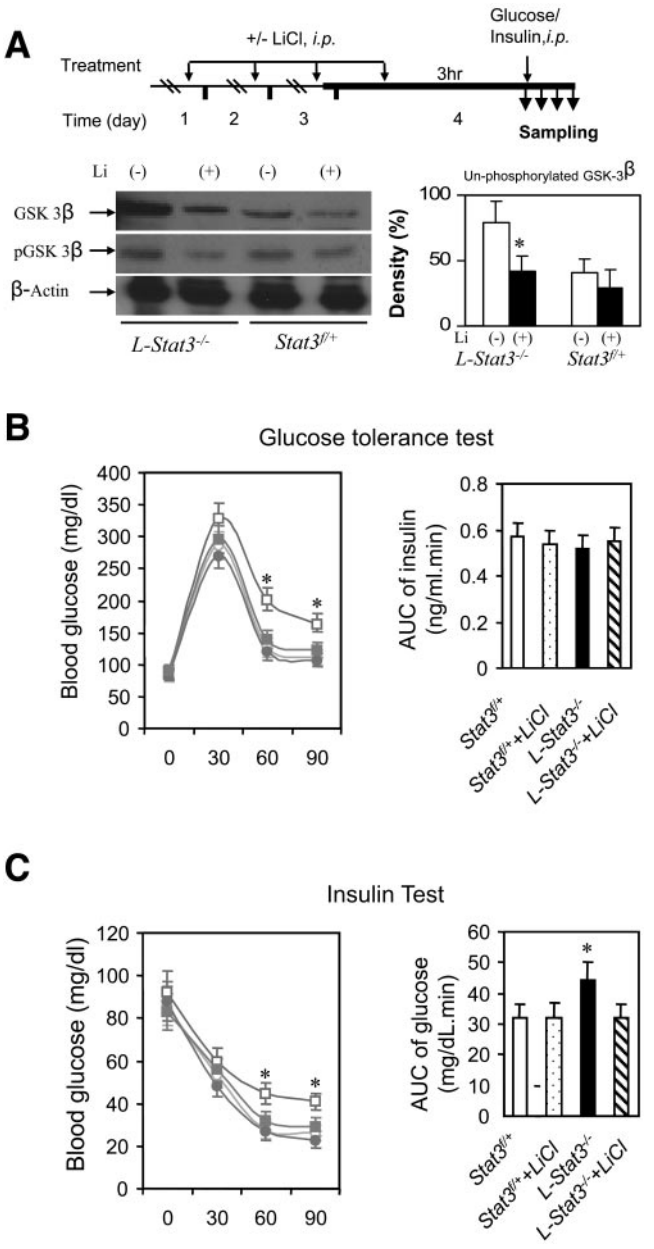

FIG. 7. Lithium chloride rescued the glucose intolerance and insulin resistance in *L-Stat3*$^{-/-}$ mice. The protocol for the rescue experiment was given in *A* with a bold horizontal line indicating "fasting." For monitoring GSK-3β, the mice were injected with 1 IU/kg insulin i.p. before and after lithium treatment, and the livers were collected to blot phosphorylated GSK-3β (pGSK-3β, serine 9) and GSK-3β (*A*, *bottom panels*). *B* and *C*: *L-Stat3*$^{-/-}$ and littermate control mice (n = 6 for each group) were pretreated with LiCl (300 mg/kg i.p.) for 4 days (*L-Stat3*$^{-/-}$+LiCl) followed by intraperitoneal injection of 2 g/kg glucose (*B*) or 1 IU/kg insulin (*C*). Blood glucose or insulin was measured at indicated time points after glucose or insulin injection. □, *L-Stat3*$^{-/-}$; ■, *L-Stat3*$^{-/-}$+LiCl; ○, *Stat3*$^{f/+}$; and ●, *Stat3*$^{f/+}$+LiCl. *P < 0.05, *L-Stat3*$^{-/-}$ vs. *L-Stat3*$^{-/-}$+LiCl, *Stat3*$^{f/+}$, or *Stat3*$^{f/+}$+LiCl by ANOVA.

function (e.g., activation of Akt in neurons) (17,34). In the nuclear translocation assay, low level of tyrosine phosphorylated STAT3 was observed in the nuclei but was independent of insulin (Fig. 3), which was consistent with a previous study (18). On the other hand, an early nuclear translocation of serine phosphorylated STAT3 was observed (Fig. 3). The data suggest a role of serine phosphorylated STAT3 in insulin action, which might switch the DNA-bound tyrosine phosphorylated STAT3 to an inhibition complex in the *Gsk-3β* promoter. Our data showing interaction of STAT3 with *Gsk-3β* regulator and decreased mRNA and protein levels of GSK-3β without significant changes in the serine 9 phosphorylation, which inactivates *Gsk-3β*, clearly indicate that STAT3 suppresses *Gsk-3β* expression (Figs. 4*E* and 5*A*). Because *Gsk-3β* is a constitutively active gene and because expression of *Gsk-3β* does not require an enhancer, STAT3 plays a relatively logical role in regulating *Gsk-3β* as a suppressor. In addition, STAT3 may recruit cofactors to determine whether to activate or repress a downstream gene (18,35). Although STAT3 sometimes plays different roles in biological events, the ultimate biochemical effect of activated STAT3 seems to lie in its ability to increase or decrease the transcriptional activity of previously quiescent or active genes. It would be interesting to further investigate whether Stat3 may also regulate GSK-3β mRNA and protein stability.

Fasting versus feeding and STAT3 in energy metabolism. It is interesting to note that there was a very physiological regulation of GSK-3β in the *Stat3*$^{f/+}$ mice in different conditions: fasting versus feeding. In feeding, because hepatocytes need insulin signaling to process glucose, mRNA levels of GSK-3β were reduced (compared with those in fasting; Fig. 5*A*) to allow insulin to induce glycogen synthesis. In fasting, because hepatocytes have to release glucose into the circulation, mRNA expression levels of GSK-3β were increased (compared with those in feeding; Fig. 5*A*) to block insulin to do the opposite work. The *L-Stat3*$^{-/-}$ mice lost this control and showed a monophasic response to insulin (Fig. 5*A*). Protein levels of GSK-3β showed similar patterns in feeding and fasting in the *L-Stat3*$^{-/-}$ and control mice (Fig. 5*B*; Supplemental Fig. 2). These data indicate that STAT3 is critical in regulating glucose and, more generally, in energy metabolism signaled by insulin.

Increased GSK-3β is responsible for impaired insulin signaling in *L-Stat3*$^{-/-}$ mice. Insulin induced a rapid increase in GSK-3β protein levels in both *L-Stat3*$^{-/-}$ and *Stat3*$^{f/+}$ mice 30 min after insulin injection (Fig. 5*B*). Because there were no significant differences between *L-Stat3*$^{-/-}$ and *Stat3*$^{f/+}$ mice within this short period of time, this change could not be related to STAT3. One could hardly interpret the rapid increase as a result of protein synthesis; it is most likely due to a protein-protein interaction and decrease in GSK-3β degradation for the early change (≤30 min) of insulin stimulation.

The loss of STAT3 in the liver resulted in an increase in the GSK-3β protein level (Fig. 5*B*), whereas the phosphorylation of GSK-3β remained unchanged (Fig. 5*B*). As a result, there was a net increase in unphosphorylated or active form of GSK-3β in *L-Stat3*$^{-/-}$ mice. Consistently, glycogen synthase activity decreased in the *L-Stat3*$^{-/-}$ mice (Fig. 6*C*). On the other hand, because a number of factors contribute to glycogen level in the liver, not just GSK-3β/glycogen synthase, it is not surprising that the glycogen level was not changed in the *L-Stat3*$^{-/-}$ mice (Fig. 6*B*). It is also possible that the low level of glycogen synthase activity (Fig. 6*B*) could not drive the difference between the *Stat3*$^{f/-}$ and *L-Stat3*$^{-/-}$ mice. Thus, although both insulin intolerance (Fig. 2) and decreased glycogen synthase activity (Fig. 6*B*) were present, the main phenotype of the *L-Stat3*$^{-/-}$ mice seems to be the impaired insulin action (Fig. 2) probably due to GSK-3β suppression of insulin signaling molecules like IRS-1 (4,5).

We hypothesized that the increased GSK-3β was the cause of impaired insulin signaling in the *L-Stat3*$^{-/-}$ mice because GSK-3β is a key negative regulator for insulin. We chose lithium chloride, the most commonly used GSK-3β inhibitor (28,36), to test our hypothesis. The data clearly show that the GSK-3β inhibitor rescued the impaired insulin effects on glucose in the *L-Stat3*$^{-/-}$ mice (Fig. 7), indicating that the increased GSK-3β was responsible for the impaired insulin signaling in the *L-Stat3*$^{-/-}$ mice. Additional discussion is available in the online appendix.

In conclusion, the present study provides evidence, we believe for the first time, that STAT3 sensitizes insulin signaling by down-regulating the expression of GSK-3β, a negative regulator of insulin. Because the STAT3 binding site in the GSK-3β is highly conserved in mice and humans (Fig. 4*A*), we speculate that a similar function should exist in humans and that mutations in this regulatory region should have a fundamental effect on insulin signaling. Thus, a novel genetic approach for fighting human type 2 diabetes could be developed based on our work showing that STAT3 negatively regulates GSK-3β.

ACKNOWLEDGMENTS

X.-Y.F. has received a Career Development Award from the National Institutes of Health (NIH), a pilot project from Yale Liver Center (DK-34989), and grants from the NIH (RO1-AI-34522 and RO1-AR-44906).

We deeply thank Dr. Peter Roach and Dr. Jose Irimia-Dominguez for generating the data of liver glycogen and glycogen synthase and for their valuable expertise and discussion. We also thank Lan Ji for excellent technical assistance.

REFERENCES

1. Taniguchi CM, Emanuelli B, Kahn CR: Critical nodes in signalling pathways: insights into insulin action. *Nat Rev Mol Cell Biol* 7:85–96, 2006
2. Cohen P, Frame S: The renaissance of GSK3. *Nat Rev Mol Cell Biol* 2:769–776, 2001
3. Harwood AJ: Regulation of GSK-3: a cellular multiprocessor. *Cell* 105:821–824, 2001
4. Summers SA, Kao AW, Kohn AD, Backus GS, Roth RA, Pessin JE, Birnbaum MJ: The role of glycogen synthase kinase 3beta in insulin-stimulated glucose metabolism. *J Biol Chem* 274:17934–17940, 1999
5. Eldar-Finkelman H, Krebs EG: Phosphorylation of insulin receptor substrate 1 by glycogen synthase kinase 3 impairs insulin action. *Proc Natl Acad Sci U S A* 94:9660–9664, 1997
6. Liberman Z, Eldar-Finkelman H: Serine 332 phosphorylation of insulin receptor substrate-1 by glycogen synthase kinase-3 attenuates insulin signaling. *J Biol Chem* 280:4422–4428, 2005
7. Nikoulina SE, Ciaraldi TP, Mudaliar S, Carter L, Johnson K, Henry RR: Inhibition of glycogen synthase kinase 3 improves insulin action and glucose metabolism in human skeletal muscle. *Diabetes* 51:2190–2198, 2002
8. Fu XY: A transcription factor with SH2 and SH3 domains is directly activated by an interferon alpha-induced cytoplasmic protein tyrosine kinase(s). *Cell* 70:323–335, 1992
9. Levy DE, Darnell JE Jr: Stats: transcriptional control and biological impact. *Nat Rev Mol Cell Biol* 3:651–662, 2002
10. Takeda K, Noguchi K, Shi W, Tanaka T, Matsumoto M, Yoshida N, Kishimoto T, Akira S: Targeted disruption of the mouse Stat3 gene leads to early embryonic lethality. *Proc Natl Acad Sci U S A* 94:3801–3804, 1997
11. Takeda K, Akira S: STAT family of transcription factors in cytokine-mediated biological responses. *Cytokine Growth Factor Rev* 11:199–207, 2000
12. Hirano T, Ishihara K, Hibi M: Roles of STAT3 in mediating the cell growth, differentiation and survival signals relayed through the IL-6 family of cytokine receptors. *Oncogene* 19:2548–2556, 2000
13. Darnell JE Jr: STATs and gene regulation. *Science* 277:1630–1635, 1997
14. Coffer PJ, van Puijenbroek A, Burgering BM, Klop-de Jonge M, Koenderman L, Bos JL, Kruijer W: Insulin activates Stat3 independently of p21ras-ERK and PI-3K signal transduction. *Oncogene* 15:2529–2539, 1997
15. Ceresa BP, Horvath CM, Pessin JE: Signal transducer and activator of transcription-3 serine phosphorylation by insulin is mediated by a Ras/Raf/MEK-dependent pathway. *Endocrinology* 138:4131–4137, 1997
16. Moh A, Iwamoto Y, Chai GX, Zhang SS, Kano A, Yang DD, Zhang W, Wang J, Jacoby JJ, Gao B, Flavell RA, Fu XY: Role of STAT3 in liver regeneration: survival, DNA synthesis, inflammatory reaction and liver mass recovery. *Lab Invest* 87:1018–1028, 2007
17. Levy DE, Lee CK: What does Stat3 do? *J Clin Invest* 109:1143–1148, 2002
18. Inoue H, Ogawa W, Ozaki M, Haga S, Matsumoto M, Furukawa K, Hashimoto N, Kido Y, Mori T, Sakaue H, Teshigawara K, Jin S, Iguchi H, Hiramatsu R, LeRoith D, Takeda K, Akira S, Kasuga M: Role of STAT-3 in regulation of hepatic gluconeogenic genes and carbohydrate metabolism in vivo. *Nat Med* 10:168–174, 2004
19. Inoue H, Ogawa W, Asakawa A, Okamoto Y, Nishizawa A, Matsumoto M, Teshigawara K, Matsuki Y, Watanabe E, Hiramatsu R, Notohara K, Katayose K, Okamura H, Kahn CR, Noda T, Takeda K, Akira S, Inui A, Kasuga M: Role of hepatic STAT3 in brain-insulin action on hepatic glucose production. *Cell Metab* 3:267–275, 2006
20. Wu H, Wade M, Krall L, Grisham J, Xiong Y, Van Dyke T: Targeted in vivo expression of the cyclin-dependent kinase inhibitor p21 halts hepatocyte cell-cycle progression, postnatal liver development and regeneration. *Genes Dev* 10:245–260, 1996
21. Yan C, Costa RH, Darnell JE Jr, Chen JD, Van Dyke TA: Distinct positive and negative elements control the limited hepatocyte and choroid plexus expression of transthyretin in transgenic mice. *EMBO J* 9:869–878, 1990
22. Welte T, Zhang SS, Wang T, Zhang Z, Hesslein DG, Yin Z, Kano A, Iwamoto Y, Li E, Craft JE, Bothwell AL, Fikrig E, Koni PA, Flavell RA, Fu XY: STAT3 deletion during hematopoiesis causes Crohn's disease-like pathogenesis and lethality: a critical role of STAT3 in innate immunity. *Proc Natl Acad Sci U S A* 100:1879–1884, 2003
23. Kano A, Watanabe Y, Takeda N, Aizawa S, Akaike T: Analysis of IFN-gamma-induced cell cycle arrest and cell death in hepatocytes. *J Biochem* (*Tokyo*) 121:677–683, 1997
24. Bromberg JF, Wrzeszczynska MH, Devgan G, Zhao Y, Pestell RG, Albanese C, Darnell JE Jr: Stat3 as an oncogene. *Cell* 98:295–303, 1999
25. Shang Y, Hu X, DiRenzo J, Lazar MA, Brown M: Cofactor dynamics and sufficiency in estrogen receptor-regulated transcription. *Cell* 103:843–852, 2000
26. Zhong Z, Wen Z, Darnell JE Jr: Stat3: a STAT family member activated by tyrosine phosphorylation in response to epidermal growth factor and interleukin-6. *Science* 264:95–98, 1994
27. Bandsma RH, Van Dijk TH, Harmsel At A, Kok T, Reijngoud DJ, Staels B, Kuipers F: Hepatic de novo synthesis of glucose 6-phosphate is not affected in peroxisome proliferator-activated receptor alpha-deficient mice but is preferentially directed toward hepatic glycogen stores after a short term fast. *J Biol Chem* 279:8930–8937, 2004
28. Pilcher HR: Drug research: the ups and downs of lithium. *Nature* 425:118–120, 2003
29. Lee JY, Hennighausen L: The transcription factor Stat3 is dispensable for pancreatic beta-cell development and function. *Biochem Biophys Res Commun* 334:764–768, 2005
30. Cui Y, Huang L, Elefteriou F, Yang G, Shelton JM, Giles JE, Oz OK, Pourbahrami T, Lu CY, Richardson JA, Karsenty G, Li C: Essential role of STAT3 in body weight and glucose homeostasis. *Mol Cell Biol* 24:258–269, 2004
31. Gorogawa S, Fujitani Y, Kaneto H, Hazama Y, Watada H, Miyamoto Y, Takeda K, Akira S, Magnuson MA, Yamasaki Y, Kajimoto Y, Hori M: Insulin secretory defects and impaired islet architecture in pancreatic beta-cell-specific STAT3 knockout mice. *Biochem Biophys Res Commun* 319:1159–1170, 2004
32. Cohen SE, Kokkotou E, Biddinger SB, Kondo T, Gebhardt R, Kratzsch J, Mantzoros CS, Kahn CR: High circulating leptin receptors with normal leptin sensitivity in liver-specific insulin receptor knock-out (LIRKO) mice. *J Biol Chem* 282:23672–23678, 2007
33. Sano S, Takahama Y, Sugawara T, Kosaka H, Itami S, Yoshikawa K, Miyazaki J, van Ewijk W, Takeda J: Stat3 in thymic epithelial cells is essential for postnatal maintenance of thymic architecture and thymocyte survival. *Immunity* 15:261–273, 2001
34. Alonzi T, Middleton G, Wyatt S, Buchman V, Betz UA, Muller W, Musiani P, Poli V, Davies AM: Role of STAT3 and PI 3-kinase/Akt in mediating the survival actions of cytokines on sensory neurons. *Mol Cell Neurosci* 18:270–282, 2001
35. Xiao H, Chung J, Kao HY, Yang YC: Tip60 is a co-repressor for STAT3. *J Biol Chem* 278:11197–11204, 2003
36. Phiel CJ, Wilson CA, Lee VM, Klein PS: GSK-3alpha regulates production of Alzheimer's disease amyloid-beta peptides. *Nature* 423:435–439, 2003